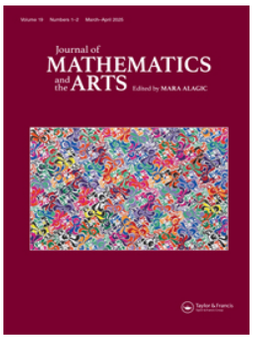

Taylor & Francis
Taylor & Francis Group

Journal of Mathematics and the Arts

ISSN: 1751-3472 (Print) 1751-3480 (Online) Journal homepage: www.tandfonline.com/journals/tmaa20

New families of monohedral polyhedra

Nina Hungerbühler, Norbert Hungerbühler & Marcel Pirron

To cite this article: Nina Hungerbühler, Norbert Hungerbühler & Marcel Pirron (2025) New families of monohedral polyhedra, Journal of Mathematics and the Arts, 19:1-2, 1-23, DOI: 10.1080/17513472.2025.2492807

To link to this article: https://doi.org/10.1080/17513472.2025.2492807

Published online: 20 May 2025.

JOURNAL OF MATHEMATICS AND THE ARTS
2025, VOL. 19, NOS. 1–2, 1–23
https://doi.org/10.1080/17513472.2025.2492807

Taylor & Francis
Taylor & Francis Group

New families of monohedral polyhedra

Nina Hungerbühler[a], Norbert Hungerbühler [b] and Marcel Pirron[b]

[a]Department of Design, Zurich University of the Arts, Zürich, Switzerland; [b]Department of Mathematics, ETH Zentrum, Zürich, Switzerland

ABSTRACT
Monohedra are polyhedra whose faces are all congruent. Since this is a very weak regularity condition, monohedra resist a rigorous classification. On the other hand, the class is particularly rich for the same reason. We show that Euler's formula nevertheless provides some simple constraints on the combinatorial possibilities of monohedra. Moreover, we describe several new infinite families of monohedra of genus 0 and genus 1. Examples of the new monohedra are staged with Blender.

ARTICLE HISTORY
Received 22 November 2022
Accepted 9 April 2025

KEYWORDS
Monohedral polyhedra; Euler's polyhedral formula; classification of polyhedra; construction methods; Blender

2020 MATHEMATICS SUBJECT CLASSIFICATIONS
52B05; 52B10

1. Introduction

In this article we explore a special class of polyhedra, the so-called monohedra. They are defined by the requirement that all their faces are congruent polygons. This is a relatively weak regularity condition, which has the consequence that the class of monohedra is mathematically difficult to grasp and has been little studied so far. For the same reason, the class is also particularly rich, which makes it interesting for creative approaches and artistic ideas. However, it is not obvious how to find construction methods to create a wide variety of monohedra to work with artistically. In our search we were able to find various new infinite families of monohedra. Our constructions are of very general nature and offer a plethora of possibilities to examine and visualize these new objects artistically. We have decided to stage the monohedra we have found with the help of *Blender*. Figure 1 shows a first example.

Blender is a free and open-source 3D computer graphics software used for modelling, sculpting, texturing, animating, and rendering. Using ray tracing technology and physical simulation of scenes, Blender delivers high-resolution photorealistic images. We encourage readers who are not yet familiar with this software to give it a try. Do not be discouraged by the initial difficulties. There are fantastic video tutorials to learn how to use the software. We carried out our calculations in a computer algebra system and exported the polyhedral data in STL format, which is readable in Blender. In the artistic realization of the

CONTACT Norbert Hungerbühler norbert.hungerbuehler@math.ethz.ch Department of Mathematics, ETH Zentrum, Rämistrasse 101, 8092 Zürich, Switzerland

Figure 1. A monohedron of genus 1, set in stage with Blender in a costal scene.

monohedra, we were inspired on the one hand by works of art or art styles and on the other hand also used the possibilities of Blender to give free rein to our imagination.

This article is organized as follows. In the next section, we briefly highlight the role of polyhedra in art and science. In order to get an overview and to categorize the monohedra in the realm of polyhedra, we outline in Section 2 the classifications that are used to approach the polyhedra mathematically. In Section 3, we explore monohedra by examining which properties they have and which laws they are subject to. This then leads us in Section 4 to new families of monohedra and to explicit construction methods. This section also features Blender-generated images of the newly discovered monohedra.

1.1. Polyhedra in art and science

Art deals with the reality that surrounds us and our imagination. Polyhedra are wanderers between these worlds. They occur in reality and play a fundamental role in the universe of ideas in mathematics. This is why polyhedra have fascinated the human mind since Egyptian and Greek antiquity. Figure 2 shows two testimonies from these eras. With their

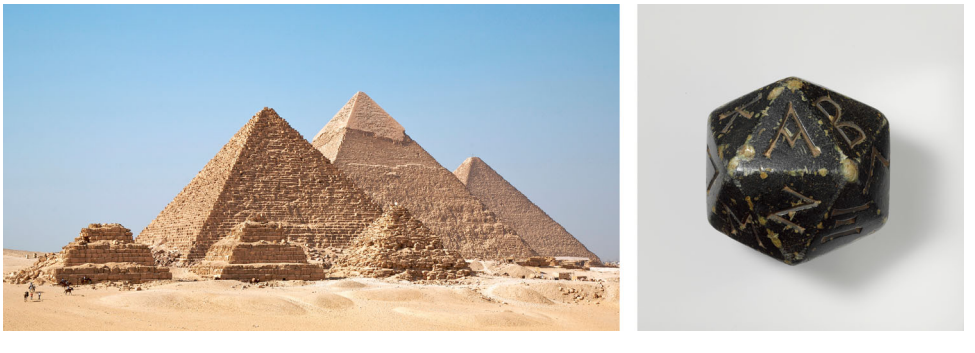

Figure 2. One the left the Giza pyramid complex (Liberato & Wikimedia Commons, 2006), on the right a greenstone icosahedron inscribed with letters of the Greek alphabet, 2nd–1st century B.C. (The Metropolitan Museum of Art, 2000–2022).

Figure 3. Pyrite Iron (II) disulfide FeS_2 forms different crystals: on the left cubic (Milla & Wikimedia Commons, 2009), in the middle dodecahedral (Descouens & Wikimedia Commons, 2011). On the right the Buckminsterfullerene C_{60} (Leyo & Wikimedia Commons, 2007).

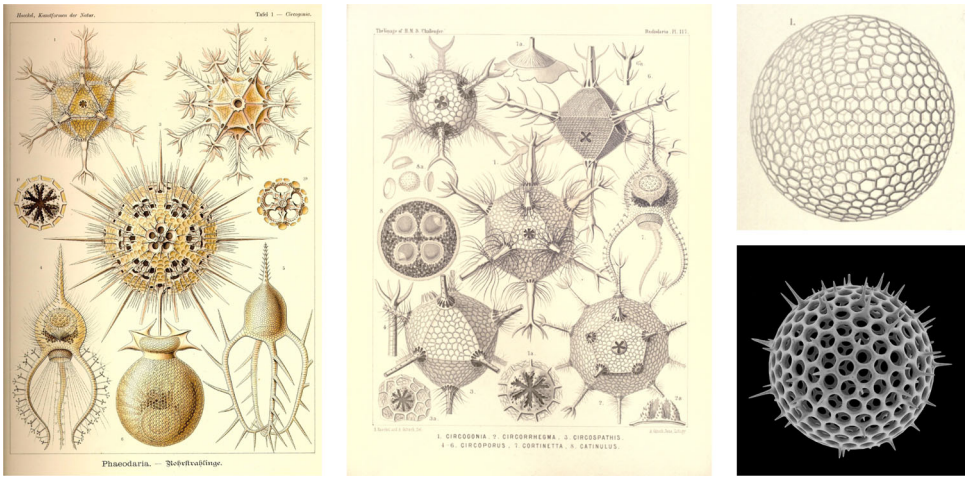

Figure 4. Radiolaria from Haeckel's books (Haeckel, 1899, Phaeodaria, Tafel 1) on the left and (Haeckel, 1887, Plate 117) in the middle. On the right a spherical radiolarian shell by Haeckel (Haeckel, 1887, Plate 111) and in a modern SEM image on the bottom (Spaw & Wikimedia Commons, 2012).

different degrees of regularity polyhedra still form a modern field of research in mathematics. On the other hand they captivate by their clear aesthetics and we wonder about their occurrence in inanimate and animate nature, as shown in Figures 3 and 4. Figure 5 illustrates that architects and designers find an inexhaustible supply of new forms and a never-ending source of inspiration in the realm of polyhedra. Polyhedra were the defining feature of the avant-garde Cubism movement at the beginning of the 20th century, which revolutionized painting and the visual arts. In his famous painting *Crucifixion (Corpus Hypercubus)*, Salvador Dalí went beyond the familiar three dimensions by depicting the crucified Christ on the polyhedron net of a hypercube.

2. Classifications of polyhedra based on their regularity

Polyhedra are among the longest and best studied mathematical objects. One of the first mathematically rigorous classifications was that of the five regular Platonic solids, which are polyhedra that satisfy the following regularity conditions.

Figure 5. The Ramot Housing Complex in Jerusalem (Hecker, 1980) top left, the Art Tower Mito (Asanagi, 2022) in Mito, Japan, top right. La Biosphère de Montréal (Daoust & Wikimedia Commons, 2015) bottom left (cropped), a classical soccer ball (Flomar & Wikimedia Commons, 2007) bottom right.

(i) All faces are regular polygons.
(ii) All faces are congruent.
(iii) The same number of faces meet at each vertex.

The only polyhedra satisfying all three regularity conditions are the tetrahedron, the hexahedron, the octahedron, the icosahedron, and the dodecahedron.

The catalogue of polyhedra becomes significantly richer if only two of the three regularity criteria are required.

- A prism of suitable height satisfies condition (i) and (iii).
- Distorted versions of the regular tetrahedron, called disphenoids (Coxeter, 1973, p. 15) satisfy condition (ii) and (iii). Disphenoids will be described in Section 4.1. In general, a polyhedron satisfying conditions (ii) and (iii) has the property that all its vertices lie on a sphere, and that another sphere can be placed inside the polyhedron, such that the sphere touches each face at its centre. A total of 12 such polyhedra are derived in Hess (1876) by Hess, who also states that this list is complete.

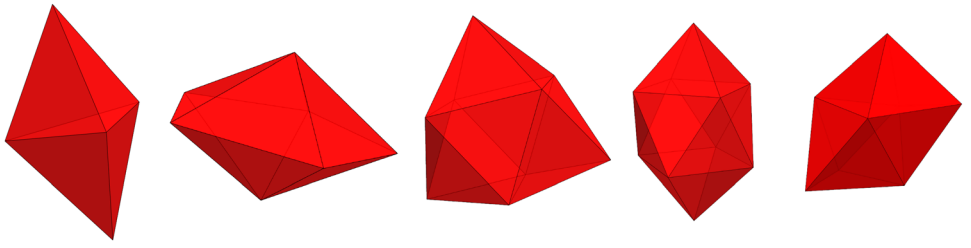

Figure 6. triangular dipyramid, pentagonal dipyramid, triaugmented triangular prism, gyroelongated square dipyramid, and siamese dodecahedron (Cromwell, 1997, p. 75).

- Apart from the Platonic solids, the convex polyhedra that satisfy (i) and (ii) are the five deltahedra[1] in Figure 6.

It is even more challenging to get an overview of the polyhedra that only fulfil one of the three regularity criteria. Only partial results are known here. Polyhedra which satisfy condition (i) and have the property that the cyclic arrangement of faces around each vertex is the same for every vertex are called semiregular. This class is completely classified (Lines, 1935): Besides the regular solids and infinitely many prisms and antiprisms, the semiregular solids consist of the thirteen Archimedean polyhedra (Waterhouse, 1972). All semiregular solids have a circumscribed sphere. The dual of a polyhedron with a circumscribed sphere is obtained in the following way: Set up the tangent plane in every vertex. Each of these tangent planes defines a half-space that contains the original polyhedron. The dual polyhedron is then the intersection of these half-spaces. The duals of the semiregular solids are called Catalan solids. Because the cyclic order of faces at each vertex of a semiregular solid is the same, their duals are composed of only one type of face. Hence Catalan solids satisfy the regularity condition (ii). This brings us to the topic we want to explore:

Definition 2.1: A *monohedron* (or *monohedral polyhedron*) is a polyhedron, such that any two of its faces are congruent. For a given monohedron M, we call any of its faces a *protogon* of M.

Since the regularity condition imposed on monohedra is very weak, their class is correspondingly rich. We are not aware of any classification of this family in the literature, not even if it is restricted to convex or starshaped monohedra. Nonetheless, we will derive in Section 3.1 some properties that are common to all monohedra and which therefore restrict the class of monohedral polyhedra. In Section 4 we will present constructions that yield some new infinite classes of monohedra.

3. Monohedral polyhedra

An important instrument for analysing polyhedra is Euler's formula. If a polyhedron P has E edges, F faces, and V vertices, then $F-E+V = 2-2g$, where g is the *genus* of P, commonly understood as the number of holes. Polyhedra that are homeomorphic to the

sphere have genus 0, torus-shaped polyhedra have genus 1, and with each additional hole the genus increases by 1.

Euler's formula alone is sufficient to show that there are only five regular Platonic solids. To see this, let $n \geq 3$ denote the number of edges of a face of a regular solid P, and $m \geq 3$ the number of edges meeting in a vertex. If we add up the edges of all faces of P we get nF which is twice the number of edges of the solid, since every edge belongs to two faces and is hence counted twice. Similarly, mV is also twice the number of edges of the solid, since every edge belongs to two vertices. Hence we have $2E = nF = mV$. Using these relations in $F - E + V = 2$, we get

$$\frac{1}{n} + \frac{1}{m} = \frac{1}{E} + \frac{1}{2} > \frac{1}{2}.$$

This inequality allows only $(3,3)$, $(3,4)$, $(3,5)$, $(4,3)$, and $(5,3)$ as possible values for (n,m) in $\mathbb{N}_{\geq 3}$, corresponding to the tetrahedron, the hexahedron, the octahedron, the icosahedron, and the dodecahedron. Notice that this derivation does not use the fact that the faces have to be regular or congruent. Only the fact that each face is bounded by the same number of sides and that at each vertex the same number of faces meet were used.

The regular Platonic solids and the five deltahedra mentioned earlier are the only convex monohedra with regular faces. As we have seen above, Catalan solids are monohedra. The family of the so called zonohedra also contains examples of monohedral polyhedra. A zonohedron is a convex, centrally symmetrical polyhedron in which each face is a centrally symmetrical polygon (a zonogon). Fedorov classified the monohedral zonohedra and found the rhombic triacontahedron, rhombic icosahedron, rhombic dodecahedron, and the infinite family of rhombohedra to be the only ones. It was only shown 75 years later that this list had to be completed by the Bilinski dodecahedron (Grünbaum, 2010). Figure 7 shows on the left that all of its protogons are congruent rhombi. It is particularly appealing that the diagonals are in the golden ratio. There is also the more restrictive concept of *isohedra*. These are monohedra such that each face can be placed at the position of any other face by a symmetry operation of the monohedron. For this reason these polyhedra make fair dice. Isohedral monohedra are completely classified (Grünbaum & Shephard, 1981). Not all monohedral zonohedra are isohedra. The Bilinski dodecahedron, for example, is not isohedral, which is apparent from Figure 7.

There exist also flexible monohedra, for example the deltahedron of Paul Mason (Cromwell, 1997, p. 222) which is shown in Figure 7 on the right.

At this point we recall the bellows theorem (Connelly et al., 1997) which states that the volume of a flexible polyhedron remains constant during the movement. Also recall that a convex polyhedron is rigid according to Cauchy's rigidity theorem (Cauchy, 1813). A rich class of flexible monohedra are the kaleidocycles, also called flextangles. They consist of an even number of tetrahedra whose faces are isosceles triangles, where two neighbouring tetrahedra are movably connected along an edge. Kaleidocycles can be continuously twisted around a ring axis. Figure 8 shows a kaleidocycle with six tetrahedra in six consecutive positions of a loop. Kaleidocycles have become popular through the Escher motifs in Schattschneider and Walker (1977), and their appearance in the 2018 science fantasy adventure film *A Wrinkle in Time*. These hinged polyhedra were examined more closely

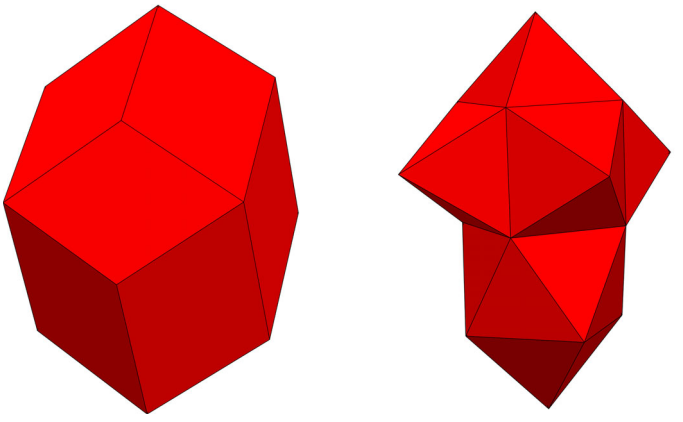

Figure 7. On the left: The Bilinski dodecahedron. It consists of twelve congruent rhombi. Four of them meet at the very top in the top vertex, and four at the very bottom in the bottom vertex. The four remaining rhombi form, in alternating orientation, a 'belt' in between. On the right: Mason's flexible monohedron. Pyramids are built on the top and around four faces of a cube. An antiprism is attached to the lower face of the cube and closed by another pyramid hanging downwards. The bottom face of the cube can then actually be slightly squeezed along the diagonal.

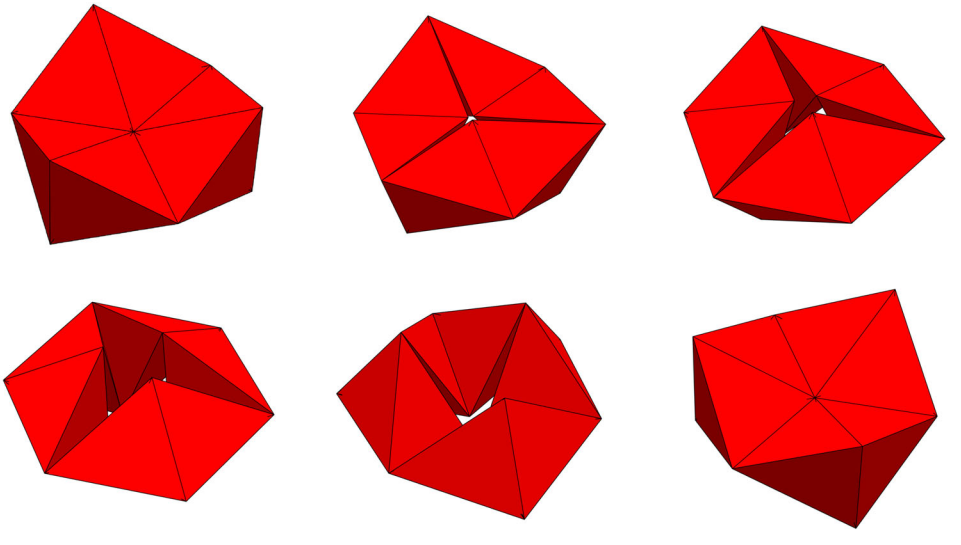

Figure 8. Twisting a kaleidocycle. The faces of the tetrahedra are isosceles triangles with side lengths $2, \sqrt{5}, \sqrt{5}$.

in Byrne (2004). The kaleidocycle in Figure 8 has $F = 24$ faces, $E = 36$ edges (the 6 edges where two tetrahedra meet are to be counted twice), and $V = 24$ vertices (all vertices belong to two tetrahedra and count twice). Formally, a kaleidocycle is therefore considered as a union of individual tetrahedra. With this convention we have $F-E+V = 12 = 2-2g$, which corresponds to a negative genus $g = -5$.

So far we have given an overview of the world of polyhedra and placed the monohedral polyhedra within it. Now we have the necessary terms and tools to derive and analyse some

properties of monohedra in the next section. This will then help in Section 4 to generate new families of monohedra.

3.1. Properties of monohedra

At this point it is worth to deliberate on the theoretical properties of monohedra. The aim is to identify general properties of monohedra in order to exclude certain combinatorial or topological variants. These findings also help in the quest for new monohedra. Already Euler's formula will impose strong restrictions on the number of faces, edges, and vertices monohedra may have. This purely topological argument also allows to show that any genus 0 monohedron is made of triangles, quadrilaterals or pentagons. Building on these findings, we will construct new monohedra in Section 4.

The prime tool in the classification of different types of polyhedra is the already mentioned formula of Euler. In the case of the regular and semiregular solids one can exploit the fact that the number of edges meeting at any vertex m is constant. At first sight it may appear as if this prevents the use of Euler's formula in the case of monohedra, since m may vary from vertex to vertex. However, a slight modification will allow its usage:

Definition 3.1: Let M be a monohedron with vertex set V, and $v \in V$. We define m_v as the number of edges meeting at v. Then, we define

$$m := \frac{1}{|V|} \sum_{v \in V} m_v$$

to be the *mean vertex type* of M.

Although the value of the mean vertex type m of a monohedron is in general not an integer (see the example below), we have similar to the case of the regular Platonic solids the following.

Lemma 3.2: *For any monohedron M whose faces are n-gons and which has mean vertex type m, E edges, F faces, and V vertices we have*

$$nF = 2E \quad \text{and} \quad mV = 2E. \tag{1}$$

Vice versa, the mean vertex type of a monohedron with V vertices and E edges is $m = \frac{2E}{V}$.

Before we come to the proof, let us illustrate the lemma using the example of the Bilinski dodecahedron. It has $V = 14$ vertices, $E = 24$ edges, and $F = 12$ faces. There are 8 vertices where 3 edges meet, and 6 vertices where 4 edges meet. The mean vertex type is therefore $m = (8 \times 3 + 6 \times 4)/14 = 24/7$. The faces are rhombi, hence $n = 4$. And indeed, we have $nF = 4 \times 12 = 48$, $mV = \frac{24}{7} \times 14 = 48$, and $2E = 2 \times 24 = 48$.

Proof of Lemma 3.2.: Any face has n edges belonging to it and every edge belongs to two faces, so $nF = 2E$. For the second relation, note that

$$mV = \sum_{v \in V} m_v.$$

The sum on the right counts every face n times. Thus we get $mV = nF = 2E$, as desired. Alternatively we can say that m_v is also the number of edges meeting in v. Therefore the sum on the right counts every edge twice, leading again to $mV = 2E$. ■

From the relation $nF = 2E$ we now get the following result which shows that any concept for constructing monohedra from triangles or pentagons with an odd number of faces is bound to fail.

Corollary 3.3: *If n is odd, any monohedron whose faces are n-gons has an even number of faces.*

By Theorem 3.4 below, genus 0 monohedra must have triangular, quadrangular or pentagonal faces. This shows that for genus 0 only monohedra with quadrilaterals as faces can potentially have an odd number of faces. It is a deep result of Grünbaum (1960) that all *convex* monohedra must have an even number of faces.

Let us now explore the restrictions for monohedra resulting from Euler's formula

$$V - E + F = 2 - 2g \tag{2}$$

for polyhedra of genus g. Using the relations in Lemma 3.2 we obtain from (2)

$$\frac{1}{m} + \frac{1}{n} = \frac{1}{2} + \frac{1-g}{E}. \tag{3}$$

This leads to the following result that provides clear numerical bounds for the number of vertices, edges and faces of monohedra.

Theorem 3.4: *Let M be a monohedron of genus $g \leq 0$. Then M has triangular, quadrangular, or pentagonal faces, with the following restrictions:*

(a) *If the faces of M are triangles, then $E \geq 6(1-g)$, $F \geq 4(1-g)$, $V \geq 4(1-g)$, and $m < 6$.*
(b) *If the faces of M are quadrilaterals, then $E \geq 12(1-g)$, $F \geq 6(1-g)$, $V \geq 8(1-g)$, and $m < 4$.*
(c) *If the faces of M are pentagons, then $E \geq 30(1-g)$, $F \geq 12(1-g)$, $V \geq 20(1-g)$, and $m < \frac{10}{3}$.*

Proof: Since $m \geq 3$ it follows from (3) that

$$\frac{1}{6} + \frac{1-g}{E} \leq \frac{1}{n}. \tag{4}$$

For $g \leq 0$, this imples $n < 6$. On the other hand, by (3), we have

$$m = \frac{2En}{E(n-2) + 2n(1-g)} \geq 3. \tag{5}$$

From this it follows

$$E \geq \frac{6n(1-g)}{6-n}$$

which gives the lower bounds for E in (a)–(c). On the other hand, the expression for m in (5) is monotonically increasing in E with supremum 6, 4, and $\frac{10}{3}$ for $n = 3, 4$, and 5, respectively. These are the upper bounds for m. The lower bounds for F and V follow subsequently from (1) and (2). ■

Notice that for genus $g \leq 0$ any three of the values V, E, F, n, m, g determine the other three by (1) and (2). For example, we can express the values of V, E, and m by F, n, and g:

Theorem 3.5: *Let M be a monohedron of genus $g \leq 0$.*

(a) *If the faces of M are triangles, then $E = \frac{3F}{2}$, $V = \frac{F}{2} + 2(1-g)$, $m = \frac{6F}{F+4(1-g)}$.*
(b) *If the faces of M are quadrilaterals, then $E = 2F$, $V = F + 2(1-g)$, $m = \frac{4F}{F+2(1-g)}$.*
(c) *If the faces of M are pentagons, then $E = \frac{5F}{2}$, $V = \frac{3F}{2} + 2(1-g)$, $m = \frac{10F}{3F+4(1-g)}$.*

Recall that in general $m \geq 3$ is a rational number bounded above by Theorem 3.4. For regular solids m has an integer value: Tetrahedron, hexahedron, and dodecahedron have $m = 3$, the octahedron has $m = 4$ and the icosahedron satisfies $m = 5$. However, there are monohedra with $m \in \mathbb{N}$ which are not regular. An example of such a monohedron is given in Section 4. The reader is invited to determine the possible values for F in this case from the equations in Theorem 3.5.

Let us now consider the case of genus $g = 1$. Interestingly, in this case, m is determined by n:

Theorem 3.6: *Let M be a monohedron of genus $g = 1$ with n-gons as faces. Then $n \in \{3, 4, 5, 6\}$. Moreover, we have $m = \frac{2n}{n-2}$, $V = E(1 - \frac{2}{n})$ and $F = \frac{2E}{n}$.*

***Proof*:** For $g = 1$ the value $n = 6$ can no longer be excluded by (4). The value of m follows immediately by (3). The values of V and F are then a consequence of (1). ■

The previous considerations put strong restrictions on possible monohedra. This is useful in the task of constructing novel monohedra. It is an open question if monohedra with an odd number of quadrilateral faces exist. At least we can now exclude the value $F = 7$ in general by using the previous result in the proof of the following theorem.

Theorem 3.7: *There is no 7-faced monohedron of genus 0.*

***Proof*:** Let us assume that a 7-faced monohedron M of genus 0 exists. Then, by Theorem 3.4, the faces of M are triangles, quadrilaterals or pentagons. However, triangles and pentagons are excluded by Corollary 3.3, so M is necessarily made of quadrilaterals. Hence we have $E = 14$ by Lemma 3.2. By assumption, M has 7 faces, thus we have by Proposition 3.5 that $m = 28/9$ and $V = 9$. We will now consider the abstract graph G given by the 9 vertices and 14 edges of the monohedron M. This allows to use the tools and the language of graph theory to deduce a contradiction to our assumption.

Since every vertex v of G must satisfy $\deg(v) \geq 3$, there has to be one vertex of degree 4 and 8 vertices of degree 3. We will now show that there is no such graph with 7 faces each bounded by 4 edges.

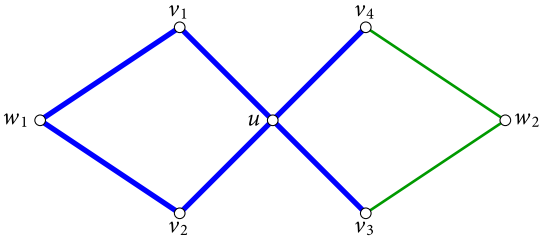

Figure 9. Local structure of *G*.

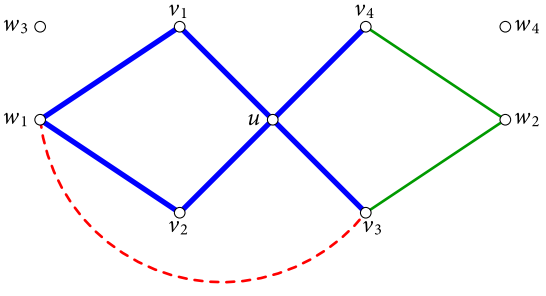

Figure 10. Local structure of *G*.

Consider a graph G satisfying the restrictions set above. Let u be the vertex of degree 4, $N = \{v_1, v_2, v_3, v_4\}$ be the set of its neighbouring vertices, and $P = \{w_1, w_2, w_3, w_4\}$ be the set of the four remaining vertices. Any edge between two vertices in N would create a triangle with u, so none of them can be in G. Any pair of direct neighbours in N has to share another neighbour in order to form a quadrilateral. Let $w_1 \neq u$ be the common neighbour of v_1 and v_2, as illustrated in Figure 9. Vertices v_3 and v_4 need to share another neighbour as well. But not w_1, because two more edges would give w_1 degree 4. So we may assume their common neighbour is w_2. The two corresponding edges are shown as thin green lines in Figure 9.

The vertices v_2 and v_3 share a neighbour as well and this might a priori be w_1 or w_2. In Figure 10 we propose w_1 with a dashed red edge, but the following argument works for w_2 as well. In both cases there need to be at least 4 edges from w_3 or w_4 to the rest of the graph. But v_1, v_2, v_4, and w_2 are the only vertices not yet saturated with edges and each of them can have only one additional edge. So all four edges go to these vertices, one edge for each vertex, and one edge has to be added between w_3 and w_4, so that they have degree 3. But then w_3 and w_4 form a path of length 5 with v_1, v_4, and u, which gives a contradiction to the assumption that the faces are quadrilaterals.

Thus v_2 and v_3 have w_3 or w_4 as common neighbour. We may assume that this is w_3. The resulting structure of G is indicated in Figure 11 with thick blue edges.

Next, we want to show, that v_1 and v_4 have w_4 as common neighbour. The only other possibilities are that their common neighbour is either w_1 or w_2. Assume it was w_1, as depicted in Figure 11, again with a dashed red edge. Then w_4 must be connected to w_2, w_3, and v_1 (dotted orange edges in Figure 11), because these are the only vertices not yet saturated. But then u, v_2, w_3, w_4, and v_1 lie on a path of length 5 and there are no edges left, giving a contradiction.

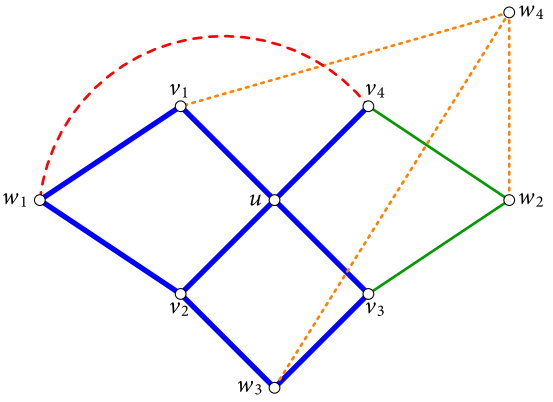

Figure 11. Local structure of G.

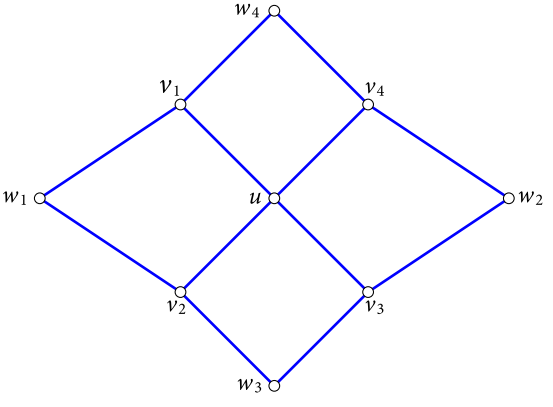

Figure 12. Local structure of G.

Thus v_1 and v_4 must have w_4 as common neighbour. This gives the structure of Figure 12.

Now each vertex of $P = \{w_1, w_2, w_3, w_4\}$ needs to be incident to one more edge, while all other vertices are saturated. Any possible configuration leads to paths of length 3 or 5 in the final graph giving again a contradiction. This shows that no graph with the given properties can exist. Therefore no monohedron with 7 faces can exist. ■

The fact that no monohedron with an odd number of faces has been found as of today could be due to a bias in the construction methods used so far: Monohedra are often only partially constructed in a first step and this part is then extended in a second step by copies of itself to form a closed monohedron. We will actually use this method in the next section. So far, these methods have led to monohedra with an even number of faces.

4. Constructions of monohedra

In the previous section we have found useful restrictions on the combinatorial structure of monohedra. When constructing novel monohedra whose sides are n-gons, one may start

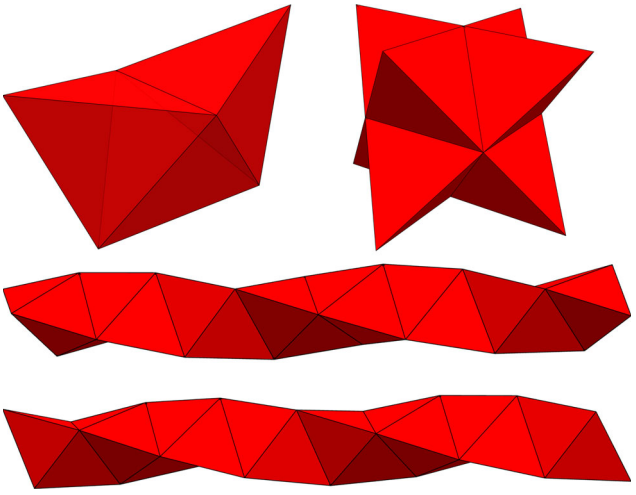

Figure 13. Top left: This monohedron, built according to Construction 1, has the same number of faces, edges, and vertices as the octahedron. Top right: The stella octangula. Bottom: The Boerdijk-Coxeter helix in two chiral forms.

by fixing the genus and the number of faces. Then all other characteristics can be determined, including m, the mean number of edges meeting in a vertex. Take, as an example, $n = 3$, $g = 0$, and $F = 6$. Then, by Theorem 3.5, we get $E = 9$, $V = 5$, and $m = 18/5$. These values are compatible with the triangular dipyramid from Figure 6: Indeed for this monohedron we have $m = \frac{1}{5}(2 \times 3 + 3 \times 4) = 18/5$. The triangular dipyramid is actually the only monohedron matching these data. To see this, observe that the only other partitions of the number $2E = 18$ with $V = 5$ integers larger than or equal to 3 are $18 = 5+4+3+3+3$ and $18 = 6+3+3+3+3$. In the first case, there would be a vertex where 5 triangles meet. However, this configuration cannot be closed with the remaining sixth triangle. And with 6 triangles around a vertex, there is no other triangle left to form a polyhedron. This shows that even with fixed values n, F, V, and thus $E = nF/2$ and $m = 2E/V$, there are in general many possibilities for distributing the edges to the vertices. In particular, there are non-congruent monohedra with the same characteristic numbers for F, E, and V. For example, the octahedron and the monohedron in Figure 13 top left have both 8 faces, 12 edges, and 6 vertices.

We start with a simple way to generate new monohedra from existing ones.

Construction 4.1: Our definition of a monohedron allows that among the faces there are the protogon and its mirror image. This is trivially the case if the protogon is mirror symmetric. Now suppose that we have a convex monohedron M that has both versions of the protogon among its faces. Then we can glue M and a copy M' of M so that two matching faces (a protogon on M and its mirror image on M') stick together exactly. More copies of M can be added in the same way. If M has only one version of the protogon (but not its mirror image) as faces, we can still glue M and its mirror image together so that the glued faces fit exactly on each other. In general, two different convex monohedra with the same protogon (or its mirror image) can be combined in this way to form a new monohedron.

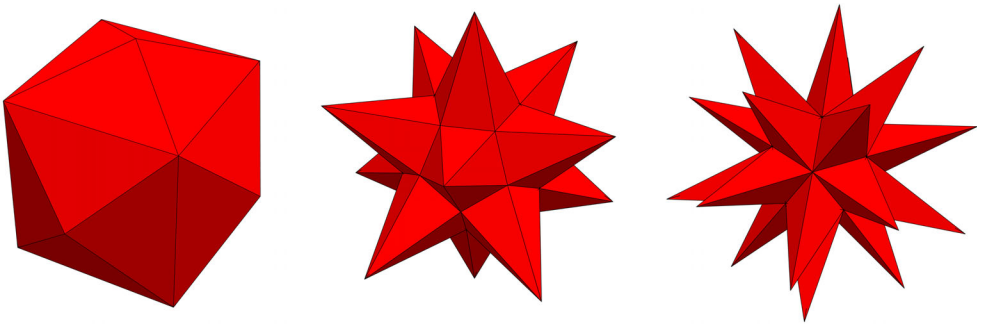

Figure 14. On the left: The tetrakis hexahedron, obtained by placing a four-sided pyramid of height 1/4 on each face of a unit cube. Middle and right: Two star polyhedra resulting from Construction 2, based on the dodecahedron and the icosahedron.

The triangular dipyramid in Figure 6 is constructed in this way by gluing two regular tetrahedra together. If another tetrahedron is glued to the triangular dipyramid, we get the monohedron in Figure 13 top left, with $F = 8$ faces, $E = 12$ edges, and $V = 6$ vertices. This is an example of a monohedron that does not satisfy the regularity condition (iii) from Section 2, but nevertheless has integer mean vertex type: $m = 2E/V = 4$. By glueing tetrahedra to each face of an octahedron creates the stella octangula in Figure 13 top right. This construction can also be used to construct monohedra that exist in two chiral forms. The best known example is the Boerdijk-Coxeter helix in Figure 13 bottom. Here, tetrahedra are glued together in such a way that the edges of the complex form three intertwined helices. The Art Tower Mito in Figure 5 is built in this particular form.

4.1. Monhedra with triangular faces

Construction 4.2: Suppose we have a convex monohedron M and suppose for simplicity that M has regular protogons. Then we may place a new vertex in the centre of each face and draw edges between each vertex of the face and its centre. If we lift each new centre vertex orthogonal to the face by the same amount, without violating the convexity of the resulting polyhedron, we obtain a new convex monohedron M' with triangular faces.

Among the Catalan solids there is an example for this construction: The tetrakis hexahedron may be obtained from the cube in this way. It is constructed by placing a pyramid with height 1/4 on each face of a unit cube. Figure 14 shows the tetrakis hexahedron and two star polyhedra which also emerge from this construction.

The construction also works for monohedra with rhombic faces (for example the aforementioned Bilinski dodecahedron), as the new vertex in the middle of each face separates the face into congruent triangles.

We can modify the previous construction in the following way.

Construction 4.3: Let M be a monohedron with an acute triangle as protogon. Observe that a nonregular monohedral tetrahedron T with the same protogon exists (a so called disphenoid or isosceles tetrahedron (Voss, 2018, Section 3)). Then we can erect a copy of

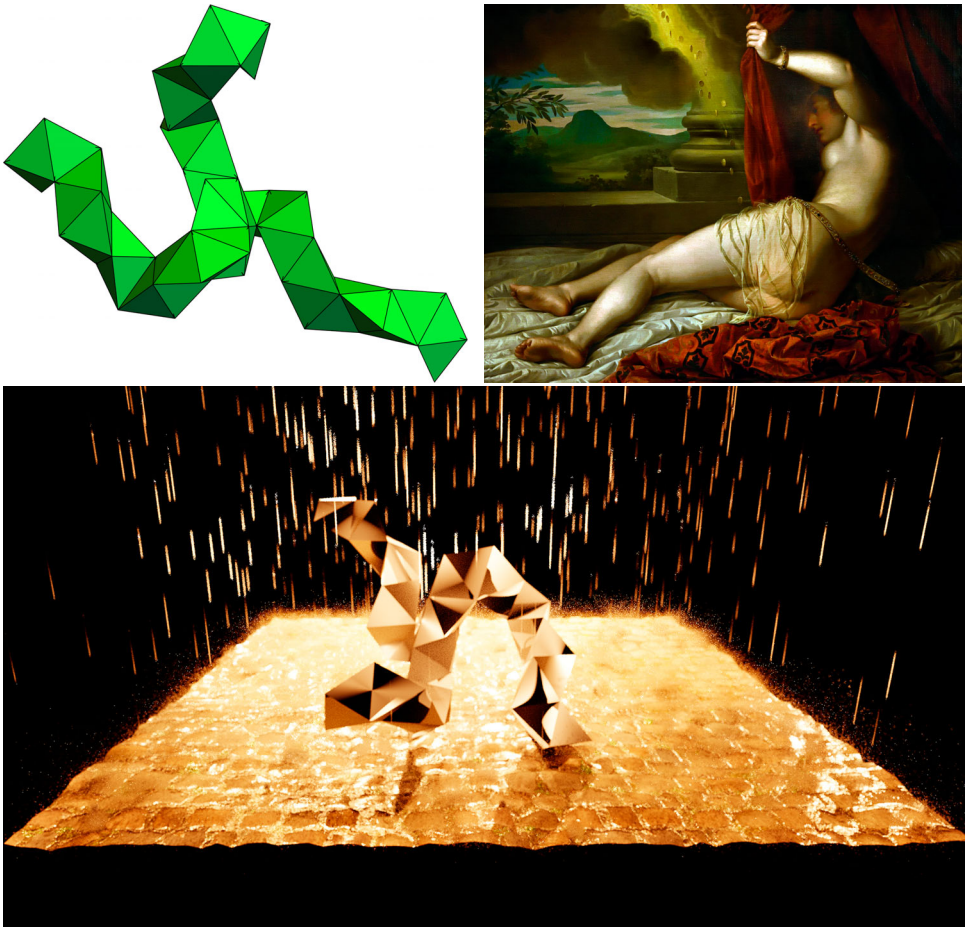

Figure 15. A monohedron with triangular faces, iteratively built by Construction 4.3, top left. The rather incidental form of the monohedron on the left reminded us vaguely of the posture of Danaë in the painting *Danae e la pioggia d'oro* top right, attributed to Giovanni Contarini, around 1570, today in the Savoy Gallery in Torino. Danaë was the only child of Eurydice and her husband Acrisius, King of Argos. Acrisius asked the oracle about male descendants, but was told that he would have no sons and that his grandson would take his life. As a result, Acrisius locked his daughter in a bronze chamber. Zeus desired Danaë and glided down to her through the roof of her prison in the form of a golden rain. Inspired by this myth we created a Blender representation of the monohedron showing the golden rain.

this disphenoid T or its mirror image on an arbitrary face of M as long as this copy does not intersect M. The result is a monohedron M' with the same protogon.

Observe that this construction can be used inductively: In each step, a new disphenoid T or its mirror image is attached to the growing monohedron, like in the example shown in Figure 15. This shows, in particular, that for any even $F \geq 4$ a monohedron with F triangular faces exists.

If M is convex, then one can erect a copy of the disphenoid T or its mirror image on each face of M. A sufficient condition that these copies do not intersect each other is, that the base point of the altitude of the disphenoid lies inside the face. As illustrated in Figure 16

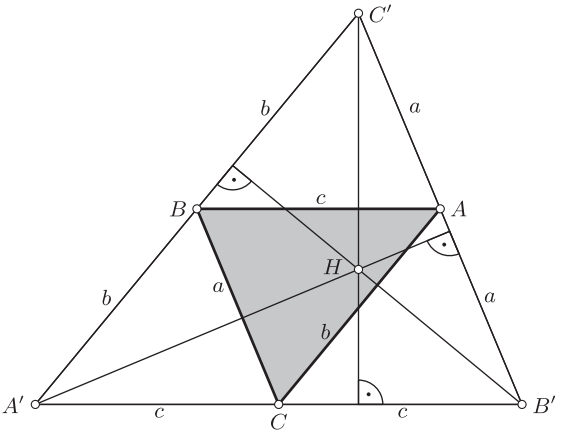

Figure 16. The net of a disphenoid with protogon *ABC* is the Gaussian extension $A'B'C'$. The triangles ABC', $A'BC$, and $AB'C$ are folded upwards along the lines *AB*, *BC*, and *AC* respectively. Then, viewed from above, the points A', B', and C' move along the altitudes until they meet in the orthocentre *H*.

it is easy to see that this is the case if and only if the orthocentre of the Gaussian extension (Hungerbühler & Wanner, 2022), (Ostermann & Wanner, 2012, Theorem 4.2), of the protogon lies inside the protogon (Voss, 2018, Section 3).

4.2. Constructing families of monohedra using coordinates

The constructions in this section are of a more systematic nature. We start with a certain idea for a combinatorial and topological design for a possible new monohedron that is compatible with the restrictions we found in Section 3.1. The vertices of the monohedron represent a set of unknown coordinates in the Euclidean space $\mathbb{R}^3$. The geometric properties of a monohedron then lead to polynomial equations for these coordinates. These equations result from two requirements.

(1) The vertices of each face of the monohedron must be coplanar. This is trivially satisfied if the protogon is a triangle. Otherwise this leads to a set of linear equations.
(2) All faces are supposed to be congruent, which means that corresponding sides and diagonals have the same length in each face. This leads to quadratic equations.

Before setting up these equations, and certainly before checking if the corresponding system of equations has a chance to have a solution, we can check if the conditions from Section 3.1 are satisfied. If not, the design will fail to give a new monohedron. In other words, it is easier to find new monohedra if we know where to look and where the search is pointless. This is how the following two constructions came about. The first one yields two new infinite families of monohedra of genus 1 with triangular faces, the second an infinite family of monohedra of genus 0 with quadrangular faces.

Construction 4.4: We start with a regular n-antiprism of height $2h > 0$ (see Figure 17 on the left). The two regular n-gons are placed in the planes $x_3 = \pm h$ and centred around the

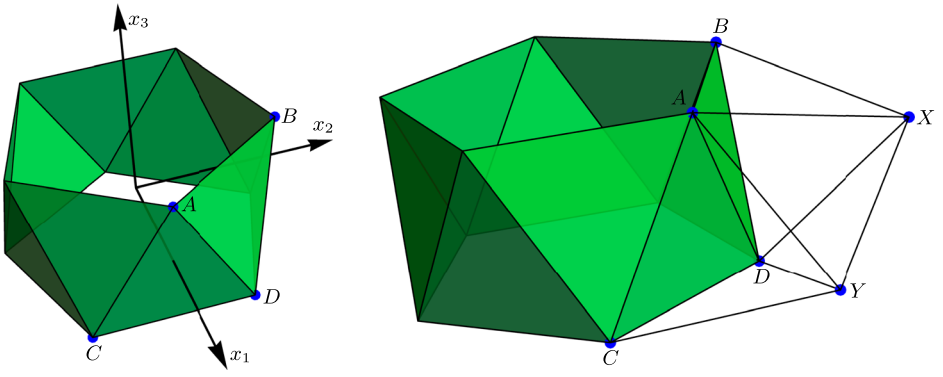

Figure 17. Left: A regular 5-antiprism as base for a monohedron of genus 1. Right: Placement of the vertices X and Y.

x_3-axis. The points A, B, C, D have the coordinates

$$A = (1, 0, h), \quad B = \left(\cos\frac{2\pi}{n}, \sin\frac{2\pi}{n}, h\right), \quad C = \left(\cos\frac{\pi}{n}, -\sin\frac{\pi}{n}, -h\right),$$
$$D = \left(\cos\frac{\pi}{n}, \sin\frac{\pi}{n}, -h\right).$$

We now locate two vertices X and Y, as shown in Figure 17 on the right, with coordinates

$$X = (x_1, x_2, x_3), \quad Y = (y_1, y_2, y_3).$$

We place X and Y in such a way that the following distances are equal:

$$|AD| = |AX| = |BX| = |CY| = |DY| = |XY|, \quad |AB| = |DX| = |AY| \tag{6}$$

By rotating Y around the x_3-axis by an angle of $\frac{2\pi}{n}$ we get a point Z. Then, by construction, the triangles CDA, ABD, ABX, AYX, DXY, CDY, BZX, and DXZ are congruent isosceles triangles. These faces are now rotated by the angles $\frac{2k\pi}{n}$, $k = 1, 2, \ldots, n-1$, around the x_3-axis to form a genus 1 monohedron.

Figure 18 shows several examples from this family of genus 1 monohedra. For $n \geq 5$ there are two solutions for the pair X, Y, one outside the antiprism, one inside. The solution for $n = 3$, which was found by a computer algebra system, is

$$X = \left(\tfrac{1}{2} + \tfrac{1}{\sqrt{2}}, \tfrac{1}{2}(\sqrt{3} + \sqrt{6}), \tfrac{1}{4}(1 - \sqrt{2})\right)$$
$$Y = \left(\sqrt{2} + 1, 0, \tfrac{1}{4}(\sqrt{2} - 1)\right)$$
$$h = \tfrac{1}{4}(\sqrt{2} + 3).$$

The expressions for larger values of n get rather unpleasant. For $n \geq 7$ we used numerical methods to compute the solutions.

We sketch the proof that the system of Equations (6) has a solution outside the antiprism for any $n \geq 3$ (the argument for the solution inside the antiprism for $n \geq 5$

Figure 18. The pictures show genus 1 monohedra for $n = 3$, 4, and 15. The last one shows an interior solution for $n = 7$. The corresponding exterior solution is illustrated in Figure 1.

is analogous). The idea is to reformulate the system (6) into one single equation for h. Note first that $|AB| = |CD| = 2\sin\frac{\pi}{n}$ does not depend on h, and that $|AC| = |AD| = \sqrt{4h^2 - 2\cos(\frac{\pi}{n}) + 2}$. Moreover, the midpoint $P := \frac{1}{2}(C + D)$ of the segment CD is given by $P = (\cos\frac{\pi}{n}, 0, -h)$. Then the coordinates of a point $Y = (y_1, 0, y_3)$ outside the antiprism satisfying $|PY| = |PA|$ and $|AY| = |CD|$ are given as a function of h. Observe that the triangles CDA and CDY are similar isosceles triangles. Now rotate Y around the x_3 axis by the angle $\frac{\pi}{n}$ and mirror the rotated point with respect to the x_1x_2-plane to get a point X. Then the triangle ABX is also similar to the triangles CDA and CDY. The distances $f(h) := |AC|$ and $g(h) := |XY|$ are functions of h. Then (6) is satisfied if $f(h) = g(h)$. We now want to use the intermediate value theorem to show that this equation has a solution. First observe that for $h_0 = \sin\frac{\pi}{2n}\sqrt{\cos\frac{\pi}{n}}$ (this is the smallest value of h for which the point Y exists) we have

$$f(h_0) = \sqrt{1 - \cos\frac{2\pi}{n}} < \sin\frac{\pi}{n}\sqrt{2\left(1 + 4\cos\frac{\pi}{n}\right)} = g(h_0).$$

To show that $f(h) > g(h)$ for sufficiently large h, we consider the equivalent inequality $\bar{f}(h) := hf(\frac{1}{h}) > hg(\frac{1}{h}) =: \bar{g}(h)$ for small positive values of h. A computer algebra system finds for the Taylor expansion at $h = 0$

$$\bar{f}(h) = 2 + \sin^2\left(\frac{\pi}{2n}\right)h^2 + O(h^4),$$

$$\bar{g}(h) = 2 + \frac{1}{2}\left(1 - 2\cos\frac{\pi}{n} + \cos\frac{3\pi}{n}\right)h^2 + O(h^4).$$

The coefficient of h^2 in the expansion of $\bar{f}$ is positive, while the coefficient of h^2 in the expansion of $\bar{g}$ is negative. Hence we have $f(h) > g(h)$ for h large enough. Since f and

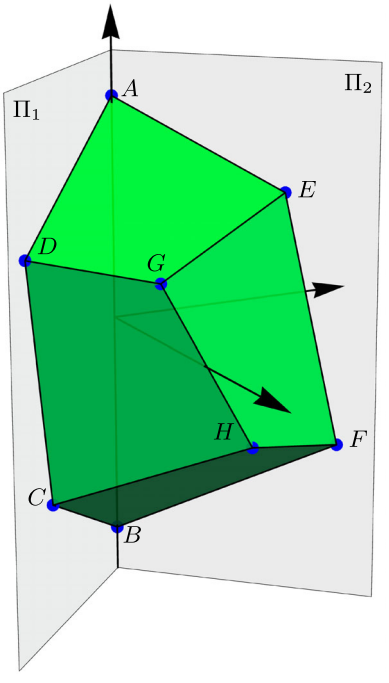

Figure 19. Construction of the monohedra with quadrangular faces.

g are continuous, the intermediate value theorem ensures the existence of a solution of $f(h) = g(h)$, which concludes the proof.

We wanted to artistically stage the monohedra we found. To do this, we used Blender to place the monohedra in different scenes, each with a specific idea. The first image at the top of Figure 18 is inspired by the steampunk television series *Arcane*. The wooden monohedron on the left could be a work of art created by Aleph Geddis. The glowing hand with the bracelet is a homage to neon art. For the last image and the image in Figure 1 we had Claude Monet's Belle-Île series, and the coastal scenes of John Brett, Winslow Homer, and Isaac Levitan in mind.

4.3. Monhedra with quadrangular faces

When constructing monohera with quadrangular faces, one must additionally introduce equations which ensure that the four vertices of a face lie in one plane. Obviously, this was not necessary for triangular faces. The idea of the following construction is, like in Construction 4, that we create only a piece of a monohedron and complete it by putting together several copies of it. More precisely, the piece we want to start with consists of four quadrilateral protogons in Figure 19, contained in a sector between two planes Π_1, Π_2 that intersect along the x_3-axis.

Construction 4.5: Let $A = (0, 0, 1)$, $B = (0, 0, -1)$, $n \geq 2$ a natural number, and $\alpha = \frac{\pi}{2n}$. We place the points D, C in the plane Π_1, E, F in the plane Π_2, and G, H inside the sector between the planes, which form an angle of $-\alpha$ and α with the positive x_1-axis. The points

are located such that the pairs (D, F), (C, E), and (G, H) are symmetric with respect to the x_1-axes. The coordinates of the points are

$$C = (t\cos\alpha, -t\sin\alpha, -u), \quad E = (t\cos\alpha, t\sin\alpha, u),$$
$$D = (r\cos\alpha, -r\sin\alpha, s), \quad F = (r\cos\alpha, r\sin\alpha, -s),$$
$$G = (x, -y, z), \quad H = (x, y, -z),$$

with real numbers r, s, t, u, x, y, z to be determined such that the quadrilaterals $ADGE$, $CDGH$ are congruent (then also $EFHG$ and $BFHC$ are congruent to the other two quadrilaterals by symmetry). Figure 19 helps to understand how these coordinates come about. Then the equations

$$|AD| = |CD|, \quad |AE| = |EG|, \quad |AE| = |HG|, \quad |AG| = |EH|, \tag{7}$$
$$\det(A - D, A - E, E - G) = 0, \quad \det(C - D, C - H, D - G) = 0 \tag{8}$$

together with

$$\frac{\det(A, D, E)}{\|(A - D) \times (A - E)\|} = \lambda \frac{\det(C, H, D)}{\|(C - H) \times (C - D)\|} \tag{9}$$

determine a monohedron with quadrangular faces: First the faces $AEGD$, $BCHF$, $CDGH$, and $EGHF$ are mirrored with respect to the plane Π_2, and then the resulting faces are rotated by angles $\frac{k\pi}{n}$, $k = 1, 2, \ldots, n-1$, around the x_3-axis.

Let us briefly comment on the Equations (7)–(9).

- The equations in (7) ensure that corresponding sides and diagonals of the four quadrilaterals have equal length.
- The equations in (8) guarantee that the faces are plane.
- The left hand side of (9) is the distance of the plane containing the quadrilateral $ADGE$ from the origin. For $\lambda = 1$, Equation (9) states that all faces have the same distance from the origin. The resulting monohedron thus has an insphere. However, λ may vary within a certain range. So, for each fixed value of n, there results an infinite family of monohedra.

The solution of the system (7)–(9) for $n = 2, \lambda = 1$, can easily be expressed by the golden ratio which is particularly pleasing: For

$$\varphi = \frac{\sqrt{5} - 1}{2}, \quad \Phi = \frac{\sqrt{5} + 1}{2}$$

we find

$$r = \frac{1}{2}\sqrt{2\Phi + 1}, \quad s = \frac{1}{2}, \quad t = \sqrt{\varphi}, \quad u = \varphi, \quad x = \sqrt{\frac{\Phi}{2}}, \quad y = \sqrt{\frac{5\varphi - 3}{2}},$$
$$z = 1 - \varphi.$$

The corresponding monohedron was apparently discovered by the Swiss architect Urs B. Roth (Waldvogel, 2019) and is described here for the first time. This monohedron is

Figure 20. The Roth monohedron with parameters $n = 2, \lambda = 1$ (top left) followed by two realizations of monohedra with quadrangular faces for $n = 3$ with $\lambda = \frac{13}{10}$ (left middle) and $\lambda = \frac{4}{5}$ (on the right), and one for $n = 9, \lambda = 1$ (bottom left, see also (Fisch, 2023) for a discussion about the making of).

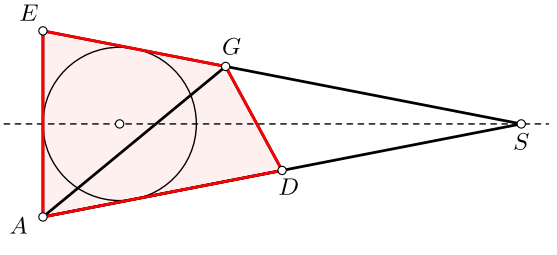

Figure 21. The protogon of the Roth monohedron. $|AE| = |EG| = 2, |GD| = \sqrt{\Phi}, |DA| = |DS| = \Phi^2, |AG| = 2\sqrt{\Phi}$.

staged in Figure 20 top right. The protogon of the Roth polyhedron has particularly nice measures if $|AE|$ is scaled to the value 2. Its geometry is illustrated in Figure 21.

Figure 20 shows examples of monohedra created by Construction 5. Here we let our imagination run freely when creating the images in Blender.

High resolution versions of the Blender images in the Figures 1, 15, 18, and 20 are available in the albums of the best scientific images of 2022 and 2023 of the Swiss National Science Foundation Swiss National Science Foundation (n.d.-a, n.d.-b). The monohedron in Figure 20, bottom left, is available as cardboard model in Christoph Pöppe's online store for polyhedra (Pöppe, 2024) under the name *Hungerbühlers Gürteltier* (Hungerbühler's Armadillo).

5. Conclusion

The constructions 4 and 5 work well for triangular and quadrangular protogons. Of course, there are also monohedra with pentagonal faces. Examples are the regular dodecahedron, the pyritohedron, the tetartoid, the pentagonal icositetrahedron and the pentagonal hexecontahedron. However, it seems difficult to extend the Constructions 4 and 5 to pentagonal faces. The reason is that not only the corresponding sides in all faces must have the same length but also two diagonals. The system of equations therefore contains more equations, which means that a possible approach must also have correspondingly more degrees of freedom. We encourage readers to make their own experiments.

Note

1. Deltahedra are polyhedra whose faces are equilateral triangles.

Acknowledgments

We are grateful to the referee for the valuable comments and suggestions that helped improve this article. We also thank the Blender community for creating and maintaining such a great 3D graphics software.

Disclosure statement

No potential conflict of interest was reported by the author(s).

ORCID

Norbert Hungerbühler http://orcid.org/0000-0001-6191-0022

References

Asanagi (2022). *Art tower mito*. Retrieved January 22, 2025, from https://commons.wikimedia.org/wiki/File:Art_Tower_Mito_2022-03-20.jpg.

Byrne, R. (2004). *Metamorphs: Transforming mathematical surprises*. Tarquin Publications.

Cauchy, A. L. (1813). Recherche sur les polyèdres – premier mémoire. *Journal de l'École Polytechnique*, *9*, 66–86.

Connelly, R., Sabitov, I., & Walz, A. (1997). The bellows conjecture. *Beiträge zur Algebra und Geometrie*, *38*(1), 1–10.

Coxeter, H. S. M. (1973). *Regular polytopes* (3rd ed.). Dover Publications, Inc.

Cromwell, P. R. (1997). *Polyhedra*. Cambridge University Press.

Daoust, F., & Wikimedia Commons (2015). *La Biosphère la nuit*. Retrieved September 9, 2024, from https://commons.wikimedia.org/wiki/File:69f9fd_4b0024cb74d54416b16ea7341d23b09f.jpg.

Descouens, D., & Wikimedia Commons (2011). *Pyrite, Rio Marina, Elba Island, Italy*. Retrieved September 9, 2024, from https://commons.wikimedia.org/wiki/File:Pyrite_elbe.jpg.

Fisch, F. (2023). Mathe in rubin. *Horizonte*, *138*, 4–5.
Flomar & Wikimedia Commons (2007). *Soccer ball*. Retrieved September 9, 2024, from https://commons.wikimedia.org/wiki/File:Soccer_ball.svg.
Grünbaum, B. (1960). On polyhedra in E^3 having all faces congruent. *Bulletin of the Research Council of Israel. Section F*, *8F*, 215–218.
Grünbaum, B. (2010). The Bilinski dodecahedron and assorted parallelohedra, zonohedra, monohedra, isozonohedra, and otherhedra. *The Mathematical Intelligencer*, *32*(4), 5–15.
Grünbaum, B., & Shephard, G. C. (1981). Spherical tilings with transitivity properties. In *The geometric vein* (pp. 65–98). Springer.
Haeckel, E. (1887). *Report on the scientific results of the voyage of H.M.S. Challenger during the years 1873–76: Vol. 18. Zoology*. Neill.
Haeckel, E. (1899). *Kunstformen der Natur*. Bibliographisches Institut, Leipzig und Wien.
Hecker, Z. (1980). The cube and the dodecahedron in my polyhedric architecture. *Leonardo*, *13*(4), 272–275.
Hess, E. (1876). Ueber die zugleich gleicheckigen und gleichflächigen Polyeder. Cassel, Th. Kay.
Hungerbühler, N., & Wanner, G. (2022). Ceva-triangular points of a triangle. *Elemente der Mathematik*, *77*(4), 180–186.
Leyo & Wikimedia Commons (2007). *Structure of the buckminsterfullerene*. Retrieved September 9, 2024, from https://commons.wikimedia.org/wiki/File:Buckminsterfullerene.svg.
Liberato, R., & Wikimedia Commons (2006). *All gizah pyramids*. Retrieved February 25, 2025, from https://en.wikipedia.org/wiki/File:All_Gizah_Pyramids.jpg.
Lines, L. (1935). *Solid geometry*. Macmillan and Co., Ltd., XX + 292.
The Metropolitan Museum of Art (2000–2022). *Greenstone polyhedron inscribed with letters of the Greek alphabet*. Retrieved September 9, 2024, from https://www.metmuseum.org/art/collection/search/252920.
Milla, C., & Wikimedia Commons (2009). *Pyrite cubic crystals on marl from Navajún, La Rioja, Spain*. Retrieved September 9, 2024, from https://commons.wikimedia.org/wiki/File:2780M-pyrite1.jpg.
Ostermann, A., & Wanner, G. (2012). *Geometry by its history*. Undergraduate Texts in Mathematics. Readings in Mathematics. Springer.
Pöppe, C. (2024). *Die Kartonbausätze – Shop*. Retrieved September 9, 2024, from http://www.poeppe-online.de/?product = hungerbuehlers-guerteltier.
Schattschneider, D., & Walker, W. (1977). *M.C. Escher Kaleidocycles*. Ballantine Books.
Spaw, M., & Wikimedia Commons (2012). *Spherical radiolarian shell*. Retrieved September 9, 2024, from https://commons.wikimedia.org/wiki/File:Spherical_radiolarian.jpg.
Swiss National Science Foundation (n.d.-a). *Scientific Image Competition, Album 2022*. Retrieved September 9, 2024, from https://www.flickr.com/photos/snsf_image_competition/albums/72177720298094208/.
Swiss National Science Foundation (n.d.-b). *Scientific Image Competition, Album 2023*. Retrieved September 9, 2024, from https://www.flickr.com/photos/snsf_image_competition/albums/72177720307215102/.
Voss, K. (2018). Tetraeder mit inhaltsgleichen Seitenflächen. *Elemente der Mathematik*, *73*(2), 45–55.
Waldvogel, J. (2019). Private communication.
Waterhouse, W. C. (1972). The discovery of the regular solids. *Archive for History of Exact Sciences*, *9*(3), 212–221.